Pandat™ 2024

Database Manual

CompuTherm LLC

PanNiobium

Database for multi-component Niobium-rich alloys

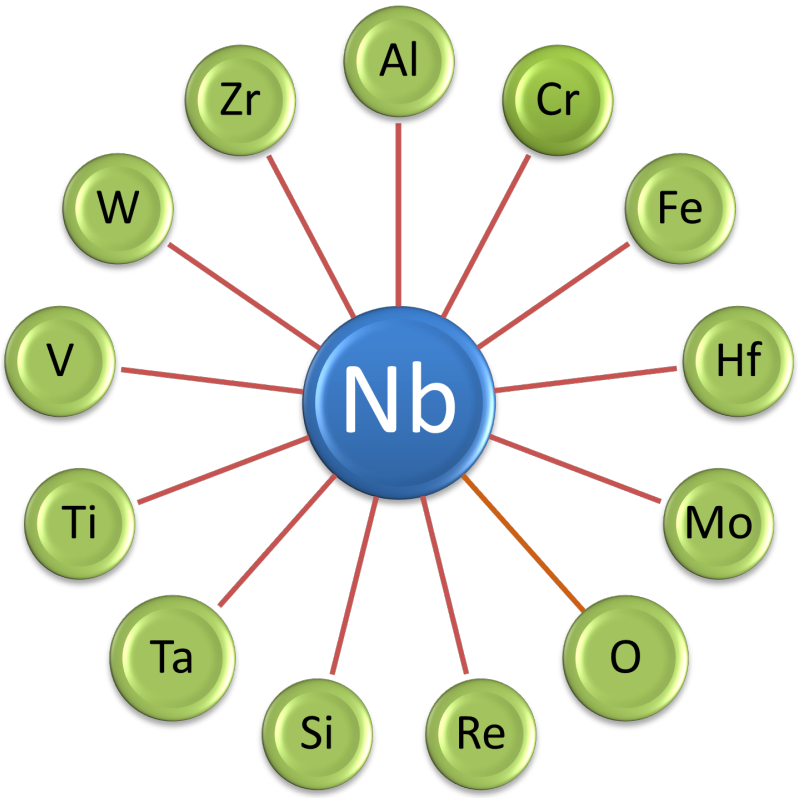

PANDAT™
SOFTWARE

Contents

1 Thermodynamic database

1.1 Components (14)

Total of **14** components are included in the database as listed here:

Al, Cr, Fe, Hf, Mo, **Nb**, O, Re, Si, Ta,Ti, V, W, and Zr

1.2 Suggested Composition Range

The suggested composition range for each element is listed in Table 1.1. It should be noted that this given composition range is rather conservative. It is derived from the chemistries of the multicomponent commercial alloys that have been used to validate the current database. In the subsystems, many of these elements can be applied to a much wider composition range. In fact, some subsystems are valid in the entire composition range as given in Section 1.5 .

Table 1.1: Suggested composition range

Elements	Composition Range (wt.%)
Nb	50 ~ 100
Si, Ti	0 ~ 30
Cr	0 ~ 20
Al, Hf, V	0 ~ 10
Fe, Mo, O, Ta, Re, W, Zr	0 ~ 5

1.3 What is new in PanNb2024

Addition of the component O

1.4 Phases

Total of **192** phases are included in the database and a few key phases are listed in Table 1.2. Information on all phases is listed in PanNb2024: List of Phases. Users can also view it through TDB viewer of Pandat™.

Table 1.2: Phase name and related information

Name	Lattice Size	Constituent
A15_Nb3Al	(0.75)(0.25)	(Cr,Fe,Hf,Mo,Nb,Si,Ti,V) (Al,Cr,Nb,Si,Ti,V)
Bcc	(1)(3)	(Al,Cr,Fe,Hf,Mo,Nb,Re,Si,Ta,Ti,V,W,Zr)(O,Va)
Chi_A12	(24)(10)(24)	(Cr,Fe,Re)(Cr,Mo,Nb,Re,Ta,Ti,W,Zr) (Cr,Fe,Mo,Nb,Re,Ta,W)
DO22	(0.25)(0.75)	(Al,Cr,Nb,Ti)(Al,Cr,Si,Ti)
Fcc	(1)(1)	(Al,Cr,Fe,Hf,Mo,Nb,Re,Si,Ta,Ti,V,W,Zr)(O,Va)
Hcp	(1)(0.5)	(Al,Cr,Fe,Hf,Mo,Nb,Re,Si,Ta,Ti, V,W,Zr)(O,Va)
Laves_C14	(2)(1)	(Al,Cr,Fe,Hf,Mo,Nb,Re,Si,Ta,Ti,V,Zr) (Al,Cr,Fe,Hf,Mo,Nb,Re,Ta,Ti,V,W,Zr)
Laves_C15	(2)(1)	(Al,Cr,Hf,Mo,Nb,Ta,Ti,V,W,Zr) (Al,Cr,Hf,Mo,Nb,Ta,Ti,V,W,Zr)
Liquid	(1)	(Al,Cr,Fe,Hf,Mo,Nb,O,Re,Si,Ta,Ti,V,W,Zr,Al2O3, Cr2/3O,FeO,FeO3/2,HfO2,MoO2,MoO3,NbO, NbO2,Nb2O5,SiO2,Ta2O5,TiO,TiO3/2,TiO2, VO,VO2,VO3/2,VO5/2,WO2,WO3,Zr1/2O)

Name	Lattice Size	Constituent
Mu_Phase	(1)(2)(4)(6)	(Fe,Mo,Nb,Ta,W)(Fe,Mo,Nb,Ta,W) (Fe,Mo,Nb,Ta,Ti,W)(Fe,Mo,Ta,W)
Nb5Si3	(0.625) (0.375)	(Cr,Hf,Nb,Ti,V,Zr)(Al,Si)
Sigma	(8)(4)(18)	(Al,Fe,Re,Si,Ta,Ti) (Cr,Fe,Mo,Nb,Ta,V,W) (Al,Cr,Fe,Mo,Nb,Re,Si,Ta,Ti,V,W)
Si3Ti5	(3)(5)	(Si)(Cr,Fe,Hf,Mo,Nb,Ti,V,Zr)

1.5 Assessed Subsystems

A total of **113** subsystems, including 89 binary and 24 ternary subsystems have been assessed. The modeling status is indicated by numbers. The systems with number 10 are fully assessed in the whole composition range. The higher value shows higher reliability of the system.

Binary Systems (89)

Al-Cr(10)	Al-Fe(10)	Al-Hf(10)	Al-Mo(10)	Al-Nb(10)	Al-O(10)	Al-Re(10)
Al-Si(10)	Al-Ta(10)	Al-Ti(10)	Al-V(10)	Al-W(10)	Al-Zr(10)	Cr-Fe(10)
Cr-Hf(10)	Cr-Mo(10)	Cr-Nb(10)	Cr-O(10)	Cr-Re(10)	Cr-Si(10)	Cr-Ta(10)
Cr-Ti(10)	Cr-V(10)	Cr-W(10)	Cr-Zr(10)	Fe-Hf(10)	Fe-Mo(10)	Fe-Nb(10)
Fe-O(10)	Fe-Re(10)	Fe-Si(10)	Fe-Ta(10)	Fe-Ti(10)	Fe-V(10)	Fe-W(10)
Fe-Zr(10)	Hf-Mo(10)	Hf-Nb(10)	Hf-O(10)	Hf-Re(10)	Hf-Si(10)	Hf-Ta(10)
Hf-Ti(10)	Hf-W(10)	Hf-Zr(10)	Mo-Nb(10)	Mo-O(10)	Mo-Re(10)	Mo-Si(10)
Mo-Ta(10)	Mo-Ti(10)	Mo-V(10)	Mo-W(10)	Mo-Zr(10)	Nb-O(10)	Nb-Re(10)
Nb-Si(10)	Nb-Ta(10)	Nb-Ti(10)	Nb-V(10)	Nb-W(10)	Nb-Zr(10)	O-Re(5)
O-Si(10)	O-Ta(10)	O-Ti(10)	O-V(10)	O-W(10)	O-Zr(10)	Re-Si(10)

Re-Ta(10)	Re-Ti(10)	Re-W(10)	Re-Zr(10)	Si-Ta(10)	Si-Ti(10)	Si-V(10)
Si-W(10)	Si-Zr(10)	Ta-Ti(10)	Ta-V(10)	Ta-W(10)	Ta-Zr(10)	Ti-V(10)
Ti-W(10)	Ti-Zr(10)	V-W(10)	V-Zr(10)	W-Zr(10)		

Ternary Systems (24)

Al-Nb-Ti(10)	Cr-Fe-Si(10)	Cr-Hf-Si(10)	Cr-Nb-Si(10)	Cr-Nb-Ti(10)	Cr-Nb-V(10)
Cr-Nb-Zr(10)	Cr-Si-Ti(10)	Cr-Si-V(10)	Cr-Ti-Zr(10)	Fe-Nb-Ti(10)	Hf-Nb-Si(10)
Hf-Nb-Zr(10)	Hf-Si-Ti(10)	Mo-Nb-Re(10)	Mo-Nb-W(10)	Mo-Si-Ti(10)	Nb-Re-Zr(10)
Nb-Si-Ti(10)	Nb-Si-W(10)	Nb-Ta-Zr(10)	Re-Ti-Zr(10)	Ta-Ti-Zr(10)	Ta-V-W(10)

1.6 Database Validation

The current PanNb database was validated by large amounts of phase equilibrium data available for Nb alloys. A few examples are given here. Figure 1.1 shows the calculated liquidus projection of the Nb-Ti-Si system together with the experimental data [1997Bew]. The different symbol of experimental data denotes that the primary solidification phase observed in the as-cast microstructure of the alloy. The two invariant reactions at the metal-rich region of Nb-Ti-Si are L+Nb5Si3 →Ti5Si3+Nb3Si at 1599 °C and L+Nb3Si → Ti5Si3+Bcc at 1359 °C.

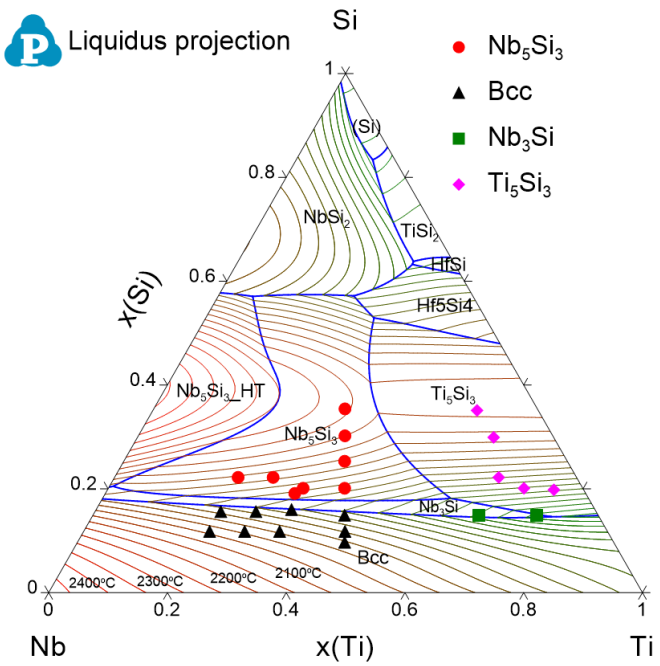

Figure 1.1: Calculated liquidus projection of Nb-Ti-Si together with experimental data [1997Bew]

Figure 1.2 and Figure 1.3 show the calculated isothermal section of Nb-Ti-Si at 1500 °C and 1340 °C, respectively. The experimental data are also plotted for comparison. The phase compositions are from EPMA measurements. The detail of experiments can be found in literature [1998Bew]. Different shapes of the symbols denote the different phase regions where the alloys are located. The green lines are tie lines.

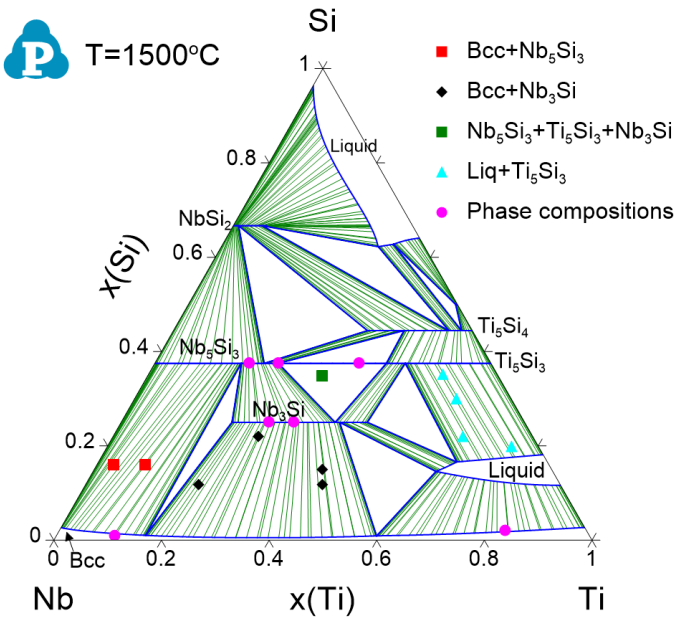

Figure 1.2: Calculated isothermal section of Nb-Ti-Si at 1500 °C together with experimental data [1998Bew]

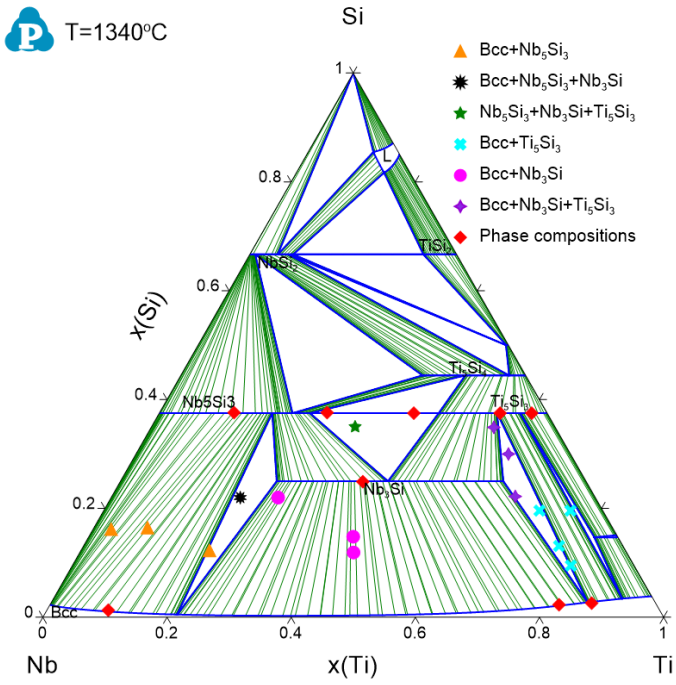

Figure 1.3: Calculated isothermal section of Nb-Ti-Si at 1340°C together with experimental data [1998Bew]

Figure 1.4 shows the calculated liquidus projection of Nb-Cr-Si overlaid by experimental data. Again, the different symbol of experimental data [2007Bew] denotes that the primary solidification phase observed in the as-cast microstructure of the alloy.Figure 1.5 shows the calculated isothermal section of Nb-Cr-Si at 1100 °C. In PanNb, a ternary phase $Nb_9Si_2Cr_3$, was included in the thermodynamic description of the Nb-Cr-Si system for the first time.

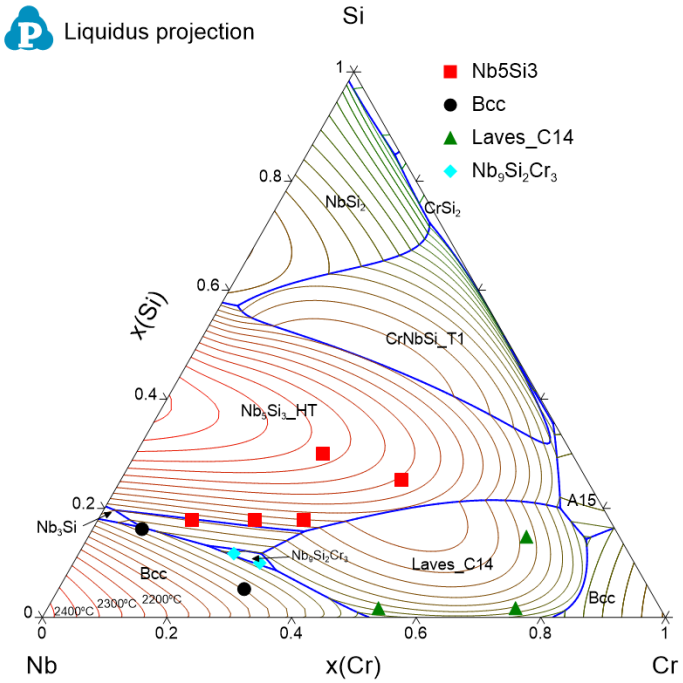

Figure 1.4: Calculated liquidus projection of Nb-Cr-Si together with experimental data [2007Bew, 2009Bew]

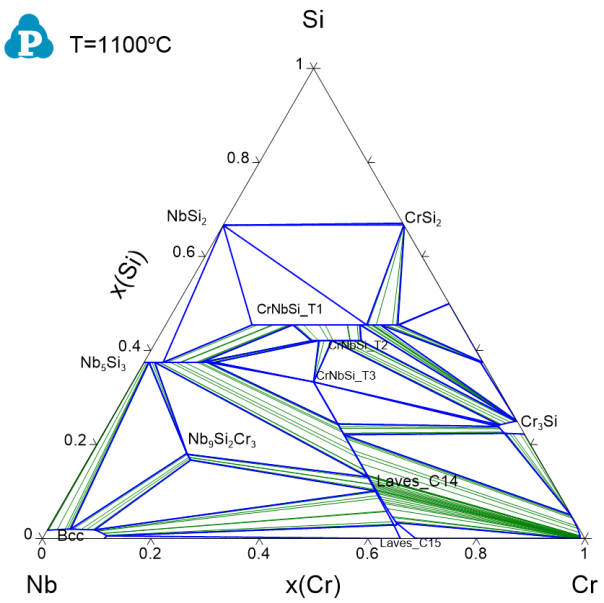

Figure 1.5: Calculated isothermal section of Nb-Cr-Si at 1100°C

Figure 1.6 shows the calculated liquidus projection of the Nb-Si-Hf overlaid by experimental data [1999Bew]. Again, the different symbol of experimental data denotes that the primary solidification phase observed in the as-cast microstructure of each alloy. The three invariant reactions at the metal-rich region of Nb-Hf-Si are L+Hf_5Si_3 → Nb_5Si_3_LT+Hf_2Si at 2035 °C, L+Nb_3Si → Nb_5Si_3_LT + Bcc at 1836 °C and L+Nb_5Si_3_LT → Hf_2Si + Bcc at 1822 °C. Figure 1.7 shows the calculated isothermal section of Nb-Hf-Si at 1500 °C together with experimental data.

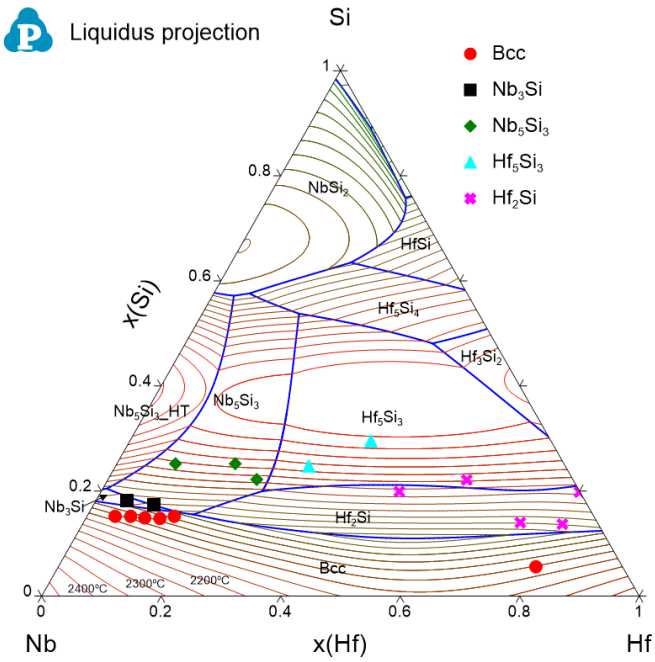

Figure 1.6: Calculated liquidus projection of Nb-Hf-Si together with experimental data [1999Bew, 2003Yan]

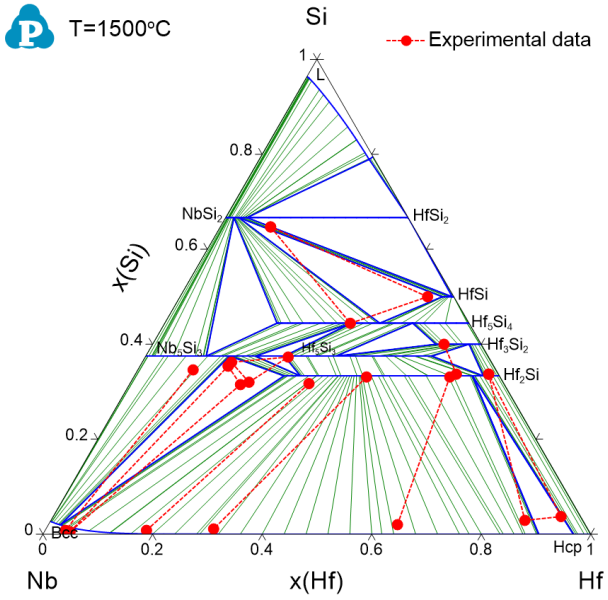

Figure 1.7: Calculated isothermal section of Nb-Hf-Si at 1500 °C together with experimental data [2001Zha]

Comparisons between the calculated phase compositions (in parentheses) and the EPMA measurements for two Nb-Cr-Ti-Si alloys are shown in Table 1.3. These measured phase compositions were not used in model parameter optimization. Instead, they were only used for validation of the calculated results. In view of this, the calculated phase compositions from the current thermodynamic description agree well with the experimental measurements. However, the users should be cautious on the discrepancy between the calculated and measured Cr and Nb compositions for the Laves_C14 phase.

Table 1.3: Comparisons between the EMPA measured and the calculated (in parentheses) phase compositions [2003Yan]

Sample	Phase	Nb (at.%)	Cr (at.%)	Ti (at.%)	Si (at.%)
Nb-10Cr-23Ti-15Si	Bcc_a2	58.2 (60.9)	13.3 (11.9)	27.4 (26.1)	1.2 (1.1)
	Nb_5Si_3	42.2 (41.5)	0.6 (1.5)	21.2 (19.5)	36.1 (37.5)
	Laves_C14	29.1 (21.9)	47.1 (55.5)	14.7 (12.7)	9 (9.9)
Nb-11Cr-23Ti-13Si	Bcc_a2	59.4 (61.2)	13.5 (12.0)	26 (25.7)	1.2 (1.1)
	Nb_5Si_3	43.7 (41.6)	0.5 (1.6)	19.5 (19.3)	36.2 (37.5)
	Laves_C14	26 (22.1)	51 (55.5)	13 (12.5)	10 (9.9)

Figure 1.8(a)-(b) show the simulated solidification paths for the Nb-11Cr-23Ti-13Si, and Nb-21Cr-23.5Ti-15.5Si alloys. The BSE images of the as-cast microstructures of these two alloys are shown in Figure 1.8(c)-(d), respectively. The phase observed in the BSE images is well predicted by the lever-rule simulation and the early stage of the Scheil simulation. The additional phases predicted by the Scheil model were not identified in the BSE images, which maybe either due to the small amount presented in the microstructure or the micro-segregation in real cooling condition is not as severe as assumed by Scheil simulation. Figure 1.9 (a) and (b) show the solidification path simulations under the Scheil and lever-rule condition for the six component Nb-22Ti-2Hf-4Cr-3Al-16Si alloy, and the BSE image of the as-cast microstructure of the same alloy. The microstructure consists of two phases (Nb) and Ti_5Si_3, which is well predicted by the lever-rule simulation as shown by the dash line in Figure 1.9 (a). The Scheil simulation predicted the formation of Ti_5Si_3 and Laves_C14 in addition to (Nb) and Ti_5Si_3. However, the total mole percentage of Ti_5Si_3 and Laves_

C14 is predicted to be less than 5%. Again, the additional phases predicted by the Scheil model were not identified in the BSE images, which maybe either due to the small amount presented in the microstructure or the micro-segregation in real cooling condition is not as severe as assumed by Scheil simulation.

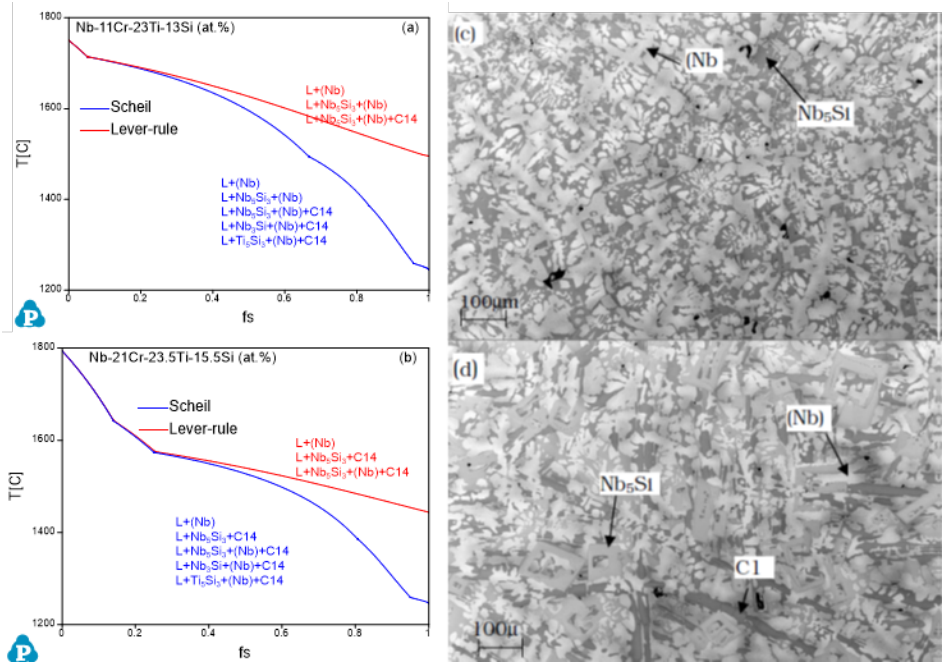

Figure 1.8: Calculated solidification paths with experimental observation (a) and (c) for alloy Nb-11Cr-23Ti-13Si; (b) and (d) for alloy Nb-21Cr-23.5Ti-15.5Si

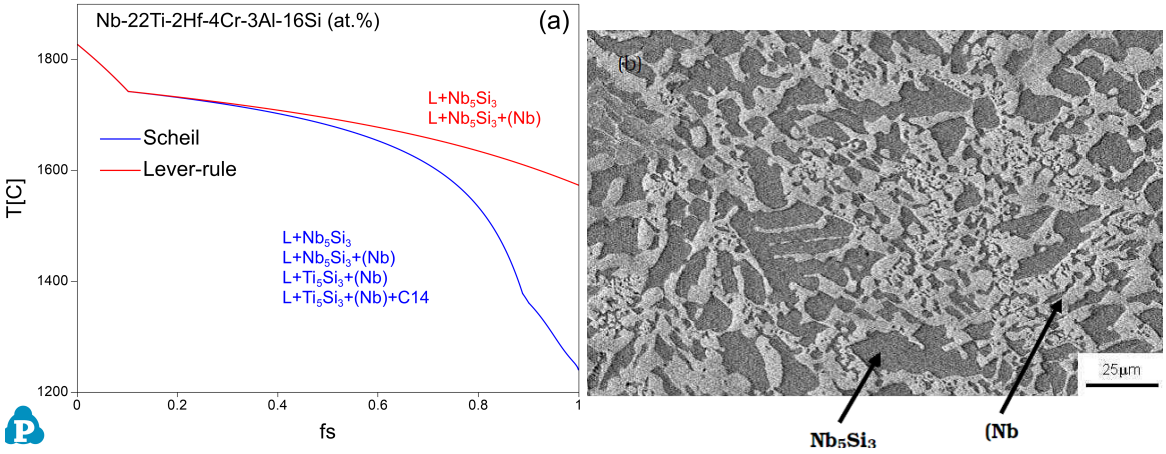

Figure 1.9: Calculated solidification path for alloys Nb-22Ti-2Hf-4Cr-3Al-16Si with experimental observation

2 Mobility Database

PanNb2024_MB is an atomic mobility database for Nb-based alloys, which is compatible with the PanNb2024_TH thermodynamic database and suitable for the simulation of diffusion-controlled phenomena using the PanDiffusion module, PanEvolution module, and/or PanSolidification module.

2.1 Phases

The atomic mobility within the **Liquid**, **Bcc**, **Fcc**, and **Hcp** solution phases are assessed in this database.

2.2 Self-diffusivity of Pure Elements

The color represents the following meaning:

: Validated
: Estimated
: No data

Table 2.1: Assessed self-diffusivity of pure elements with different crystal structures

	Al	Cr	Fe	Hf	Mo	Nb	Re	Si	Ta	Ti	V	W	Zr
Bcc													
Fcc													
Hcp													

2.3 Assessed Systems

In addition to the assessed self-diffusivities shown above, the impurity diffusion data for all elements included in the current PanNb2024_MB mobility database are also assessed. Moreover, chemical-diffusivities available in some binary and ternary systems are also used to assess the interaction parameters. These binary and ternary systems are listed below for the Bcc, Fcc, and Hcp phases, respectively.

Fcc Phase

Al-Si	Al-W	Cr-Fe	Cr-Ni	Fe-Si

Bcc phase

Al-Fe	Al-Ti	Cr-Fe	Cr-Ti	Fe-Ti	Hf-Zr	Mo-Nb	Mo-Ta	Mo-Ti	Mo-W
Mo-Zr	Nb-Ta	Nb-Ti	Nb-V	Nb-W	Nb-Zr	Ta-Ti	Ta-W	Ti-V	Ti-Zr
V-Zr									

Al-Cr-Ti	Al-Fe-Ti

2.4 Database Validation

The simulated concentration profiles of a series of Nb-based alloys are shown below to validate the current PanNb2024_MB database.

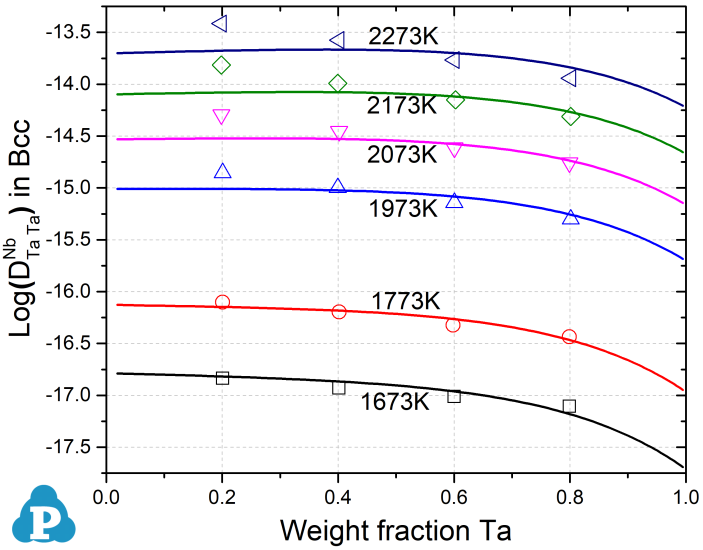

Figure 2.1: Inter-diffusion of Ta in bcc Nb-Ta alloys at different temperatures [2013Liu]

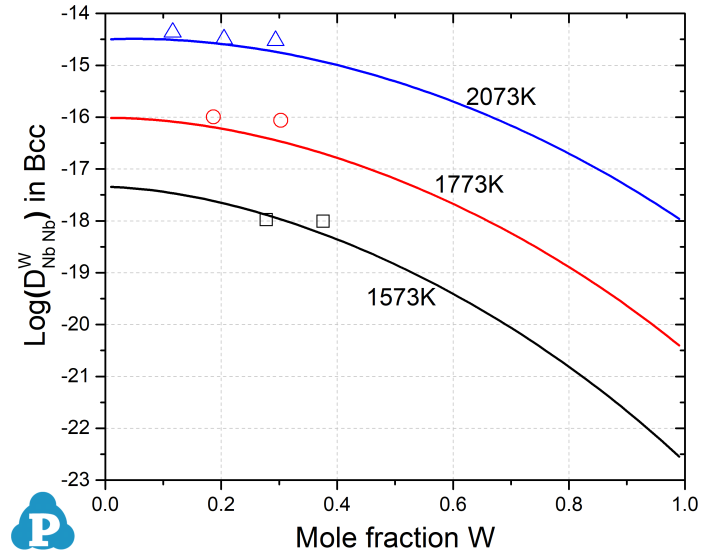

Figure 2.2: Inter-diffusion coefficients of Nb in bcc Nb-W alloys at different temperatures [2013Liu]

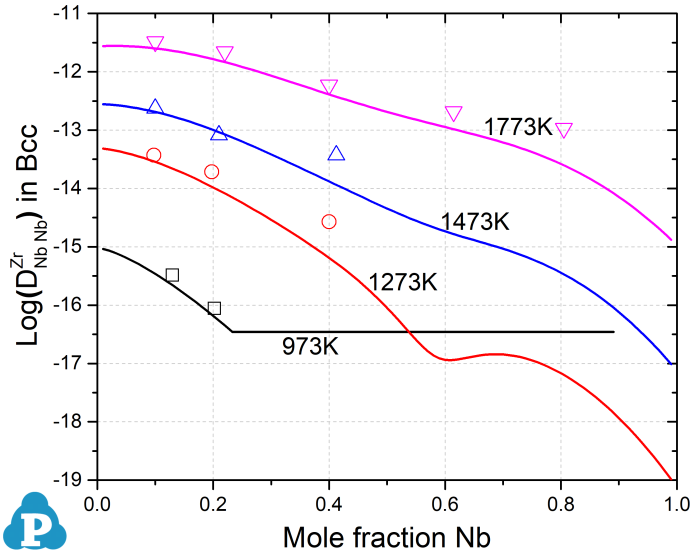

Figure 2.3: Inter-diffusion coefficients of Nb in bcc Nb-Zr alloys at different temperatures [2008Liu]

3 Thermophysical Property Database

The thermophysical property database **PanNb2024_ TP** is compatible with the `PanNb2024_TH` thermodynamic database and suitable for the simulation of thermophysical properties of Nb-based alloys. It includes the molar volume data for all the phases, surface tension and viscosity properties for the liquid phase.

3.1 Molar Volume

The current molar volume database covers all **192** phases assessed in the `PanNb2024_TH` database. It is used to calculate the density, thermal expansion, solidification shrinkage of Nb alloys.

The simulated density changes vs. temperature of a series of Nb-based alloys are shown below to validate the current `PanNb2024_MV` database.

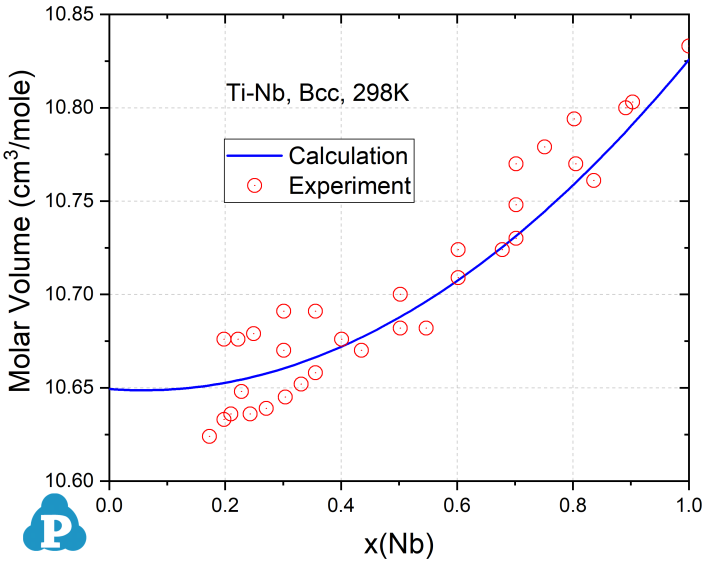

Figure 3.1: Molar volume of Nb-Ti Bcc binary alloys at 298K [2016Yan]

4 References

[1997Bew] B. P. Bewlay, M. R. Jackson, H. A. Lipsitt, Journal of Phase Equilibria, 18(3) (1997): 264-278.

[1998Bew] B. P.Bewlay, M. R. Jackson, R. R. Bishop, Journal of Phase Equilibria, 19(6) (1998): 577-586.

[1999Bew] B.P. Bewlay, R.R. Bishop, M.R.Jackson, Zeitschrift fuer Metallkunde, 90(6) (1999): 413-422.

[2001Zha] J.-C. Zhao, B.P. Bewlay, M.R.Jackson, Intermetallics, 9(8) (2001): 681-689.

[2003Yan] Y. Yang,Y. A. Chang, J.-C. Zhao, B.P. Bewlay, Intermetallics: 11(5) (2003): 407-415.

[2007Bew] B. Bewlay, P.; Y. Yang, R. L. Casey, M. R. Jackson, Y. A. Chang, Materials Research Society Symposium Proceedings, 980 (2007): 333-338.

[2008Liu] Y. Liu, et al., Study of diffusion mobilities of Nb and Zr in bcc Nb-Zr alloys. Calphad, 32 (2008): 455-461.

[2009Bew] B.P. Bewlay, Y. Yang, R. L. Caesy, M.R. Jackson Y. A. Chang, Intermetallics, 17 (3) (2009): 120-127.

[2013Liu] Y. Liu, et al., Mobilities and diffusivities for bcc Nb-W, Nb-Ta, Zr-Mo and Zr-Hf alloys. Journal of Alloys and Compounds, 555 (2013): p. 381-389.

[2016Yan] J.-Y. Yan and G.B. Olson, Molar volumes of bcc, hcp, and orthorhombic Ti-base solid solutions at room temperature. Calphad, 52 (2016): 152-158.

PanNb2024: List of Phases

Phases (**192**)

Name	Model	Lattice Size	Constituent
A15_Nb3Al	CEF (SLN)	(0.75)(0.25)	(Cr,Fe,Hf,Mo,Nb,Si,Ti,V)(Al,Cr,Nb,Si,Ti,V)
A_TiO	CEF (ST2)	(1)(1)	(Ti)(O)
Al10V	CEF (ST2)	(10)(1)	(Al)(V)
Al11Cr2	CEF (ST2)	(10)(1)(2)	(Al)(Al)(Cr)
Al11Re4	CEF (ST2)	(11)(4)	(Al)(Re)
Al12Mo	CEF (ST2)	(12)(1)	(Al)(Mo)
Al12Re	CEF (ST2)	(12)(1)	(Al)(Re)
Al12W	CEF (ST2)	(12)(1)	(Al)(W)
Al13Cr2	CEF (ST2)	(13)(2)	(Al)(Cr)
Al13Fe4	CEF (SLN)	(0.6275) (0.235) (0.1375)	(Al)(Fe)(Al,Va)
Al17Mo4	CEF (ST2)	(17)(4)	(Al)(Mo)
Al1Fe1O3	CEF (ST3)	(1)(1)(3)	(Al+3)(Fe+3)(O-2)
Al22Mo5	CEF (ST2)	(22)(5)	(Al)(Mo)
Al23V4	CEF (ST2)	(23)(4)	(Al)(V)
Al2Fe	CEF (ST2)	(2)(1)	(Al)(Fe)
Al2Hf	CEF (ST2)	(0.66667) (0.33333)	(Al)(Hf)
Al2Hf3	CEF (ST2)	(0.4)(0.6)	(Al)(Hf)

Name	Model	Lattice Size	Constituent
Al2W	CEF (ST2)	(2)(1)	(Al)(W)
Al2Zr	CEF (ST2)	(2)(1)	(Al)(Zr)
Al2Zr3	CEF (ST2)	(2)(3)	(Al)(Zr)
Al3Hf2	CEF (ST2)	(0.6)(0.4)	(Al)(Hf)
Al3Hf4	CEF (ST2)	(0.42857) (0.57143)	(Al)(Hf)
Al3Hf_alpha	CEF (ST2)	(0.75)(0.25)	(Al)(Hf)
Al3Hf_beta	CEF (ST2)	(0.75)(0.25)	(Al)(Hf)
Al3Mo	CEF (ST2)	(3)(1)	(Al)(Mo)
Al3V	CEF (ST2)	(3)(1)	(Al)(V)
Al3Zr	CEF (ST2)	(3)(1)	(Al)(Zr)
Al3Zr2	CEF (ST2)	(3)(2)	(Al)(Zr)
Al3Zr4	CEF (ST2)	(3)(4)	(Al)(Zr)
Al3Zr5	CEF (ST2)	(3)(5)	(Al)(Zr)
Al4Cr	CEF (ST2)	(4)(1)	(Al)(Cr)
Al4M	CEF (ST2)	(4)(1)	(Al)(W)
Al4Mo	CEF (ST2)	(4)(1)	(Al)(Mo)
Al4Re	CEF (ST2)	(4)(1)	(Al)(Re)
Al4Zr5	CEF (ST2)	(4)(5)	(Al)(Zr)
Al5Fe2	CEF (ST2)	(5)(2)	(Al)(Fe)
Al5Fe4	CEF (SLN)	(1)	(Al,Fe)
Al5M	CEF (ST2)	(5)(1)	(Al)(W)
Al5Mo	CEF (ST2)	(5)(1)	(Al)(Mo)
Al63Mo37	CEF (ST2)	(63)(37)	(Al)(Mo)
Al69Ta39	CEF (SLN)	(0.6389)	(Al,Ta)(Al,Ta)

Name	Model	Lattice Size	Constituent
		(0.3611)	
Al6Re	CEF (ST2)	(6)(1)	(Al)(Re)
Al77W23	CEF (ST2)	(77)(23)	(Al)(W)
Al7V	CEF (ST2)	(7)(1)	(Al)(V)
Al7W3	CEF (ST2)	(7)(3)	(Al)(W)
Al8Cr5_H	CEF (ST2)	(8)(5)	(Al)(Cr)
Al8Cr5_L	CEF (ST2)	(8)(5)	(Al)(Cr)
Al8Mo3	CEF (ST2)	(8)(3)	(Al)(Mo)
Al8V5	CEF (ST2)	(8)(5)	(Al)(V)
Al9Cr4_H	CEF (ST2)	(9)(4)	(Al)(Cr)
Al9Cr4_L	CEF (ST2)	(9)(4)	(Al)(Cr)
AlCr2	CEF (ST2)	(1)(2)	(Al)(Cr)
AlHf	CEF (ST2)	(0.5)(0.5)	(Al)(Hf)
AlHf2	CEF (ST2)	(0.33333) (0.66667)	(Al)(Hf)
AlMo3	CEF (SLN)	(1)(3)	(Al,Mo)(Al,Mo)
AlRe	CEF (ST2)	(1)(1)	(Al)(Re)
AlRe2	CEF (ST2)	(1)(2)	(Al)(Re)
AlZr	CEF (ST2)	(1)(1)	(Al)(Zr)
AlZr2	CEF (ST2)	(1)(2)	(Al)(Zr)
AlZr3	CEF (ST2)	(1)(3)	(Al)(Zr)
B2	CEF (SLN)	(0.5)(0.5)	(Fe,Ta,Ti,W)(Fe,Ta,Ti,W,Va)
BCC_B2	CEF (SLN)	(0.5)(0.5)(3)	(Al,Cr,Fe,Si,Ti)(Al,Cr,Fe,Si,Ti)(Va)
BETA_VO	CEF (SLN)	(1)(1)	(V)(O,Va)

Name	Model	Lattice Size	Constituent
BRONZE	CEF (SLN)	(2)(5)(1)	(V+4,V+5)(O-2)(Va)
Bcc	CEF (SLN)	(1)(3)	(Al,Cr,Fe,Hf,Mo,Nb,Re,Si,Ta,Ti,V,W,Zr) (O,Va)
Chi_A12	CEF (SLN)	(24)(10)(24)	(Cr,Fe,Re)(Cr,Mo,Nb,Re,Ta,Ti,W,Zr) (Cr,Fe,Mo,Nb,Re,Ta,W)
Corundum	CEF (SLN)	(2)(1)(3)	(Al+3,Cr+2,Cr+3,Fe+2,Fe+3,Ti+3, V+3,V+4,Va)(Cr+3,Fe+3,Va)(O-2)
Cr4Si3	CEF (ST2)	(4)(3)	(Cr)(Si)
CrHfSi	CEF (ST3)	(1)(1)(1)	(Cr)(Hf)(Si)
CrNbSi_T1	CEF (SLN)	(6)(5)	(Cr,Nb)(Si)
CrNbSi_T2	CEF (SLN)	(11)(8)	(Cr,Nb)(Si)
CrNbSi_T3	CEF (ST3)	(1)(1)(1)	(Cr)(Nb)(Si)
CrSi	CEF (SLN)	(1)(1)	(Cr,Fe,V)(Si)
Cristobalite	CEF (ST2)	(1)(2)	(Si)(O)
D0_22_ Al3Ta	CEF (SLN)	(0.75)(0.25)	(Al)(Al,Ta)
DO22	CEF (SLN)	(0.25)(0.75)	(Al,Cr,Nb,Ti)(Al,Cr,Si,Ti)
Diamond_A4	CEF (SLN)	(1)	(Al,Si,Ti)
Fcc	CEF (SLN)	(1)(1)	(Al,Cr,Fe,Hf,Mo,Nb,Re,Si,Ta,Ti,V,W,Zr) (O,Va)
Fe2Hf_C14	CEF (SLN)	(0.6667) (0.3333)	(Fe)(Fe,Hf)
Fe2Hf_C15	CEF (ST2)	(0.6667) (0.3333)	(Fe)(Hf)
Fe2Hf_C36	CEF (ST2)	(0.6667) (0.3333)	(Fe)(Hf)

Name	Model	Lattice Size	Constituent
Fe2Si	CEF (ST2)	(2)(1)	(Fe)(Si)
Fe2Ta3	CEF (SLN)	(2)(3)	(Fe,Ta)(Fe,Ta)
Fe2Zr_C15	CEF (SLN)	(2)(1)	(Fe,Zr)(Fe,Zr)
Fe2Zr_C36	CEF (SLN)	(2)(1)	(Fe,Zr)(Fe,Zr)
Fe4Re	CEF (SLN)	(4)(1)	(Fe,Re)(Fe,Re)
FeHf2	CEF (ST2)	(0.3333) (0.6667)	(Fe)(Hf)
FeSi2_H	CEF (ST2)	(3)(7)	(Fe)(Si)
FeSi2_L	CEF (ST2)	(1)(2)	(Fe)(Si)
FeZr2	CEF (SLN)	(1)(2)	(Al,Fe,Zr)(Zr)
FeZr3	CEF (SLN)	(1)(3)	(Al,Fe,Zr)(Fe,Zr)
GAS	GAS	(1)	(Al,AlO,AlO2,Al2,Al2O,Al2O2,Al2O3,Fe,FeO, FeO2,Fe2,Hf,HfO,HfO2,O,O2,O3,Si,Si2,Si3, SiO,SiO2,Ti,TiO,TiO2,Zr,Zr2,ZrO,ZrO2)
Halite	CEF (SLN)	(1)(1)	(Al+3,Cr+3,Fe+2,Fe+3,V,V+2,V+3,Va) (O-2,Va)
Hcp	CEF (SLN)	(1)(0.5)	(Al,Cr,Fe,Hf,Mo,Nb,Re,Si,Ta,Ti,V,W,Zr) (O,Va)
Hf2Si	CEF (SLN)	(0.666667) (0.333333)	(Cr,Hf,Nb,Ti,Zr)(Si)
Hf3Si2	CEF (SLN)	(0.6)(0.4)	(Cr,Hf,Nb,Zr)(Si)
Hf5Si4	CEF (SLN)	(0.555556) (0.444444)	(Cr,Hf,Mo,Nb,Ti,Zr)(Si)
HfSi	CEF (SLN)	(0.5)(0.5)	(Cr,Hf,Nb,Ti,Zr)(Al,Si)
HfSi2	CEF (SLN)	(0.333333) (0.666667)	(Cr,Hf,Zr)(Si)

Name	Model	Lattice Size	Constituent
HfSiO4	CEF (ST3)	(1)(1)(4)	(Hf)(Si)(O)
Laves_C14	CEF (SLN)	(2)(1)	(Al,Cr,Fe,Hf,Mo,Nb,Re,Si,Ta,Ti,V,Zr) (Al,Cr,Fe,Hf,Mo,Nb,Re,Ta,Ti,V,W,Zr)
Laves_C15	CEF (SLN)	(2)(1)	(Al,Cr,Hf,Mo,Nb,Ta,Ti,V,W,Zr) (Al,Cr,Hf,Mo,Nb,Ta,Ti,V,W,Zr)
Laves_C36	CEF (SLN)	(2)(1)	(Cr,Zr)(Cr,Zr)
Liquid	CEF (SLN)	(1)	(Al,Cr,Fe,Hf,Mo,Nb,O,Re,Si,Ta,Ti,V,W,Zr, Al2O3,Cr2/3O,FeO,FeO3/2,HfO2,MoO2, MoO3,NbO,NbO2,Nb2O5,SiO2,Ta2O5, TiO,TiO3/2,TiO2,VO,VO2,VO3/2,VO5/2, WO2,WO3,Zr1/2O)
M11Si8	CEF (SLN)	(11)(8)	(Cr,V)(Si)
M6Si5	CEF (SLN)	(6)(5)	(Cr,Ti)(Si)
MSi2	CEF (SLN)	(1)(2)	(Cr,Hf,Mo,Nb,Si,Ti,V)(Al,Cr,Si)
Mo2Hf	CEF (SLN)	(2)(1)	(Hf,Mo)(Hf,Mo)
Mo4O11	CEF (ST2)	(0.266667) (0.733333)	(Mo)(O)
Mo4Si9Ti7	CEF (SLN)	(0.55)(0.45)	(Mo,Ti)(Si)
Mo5Si3	CEF (SLN)	(0.625) (0.375)	(Cr,Fe,Hf,Mo,Nb,Si,Ti,W,Zr)(Al,Mo,Nb,Si)
Mo8O23	CEF (ST2)	(0.258064) (0.741935)	(Mo)(O)
Mo9O26	CEF (ST2)	(0.257143) (0.742857)	(Mo)(O)
MoO3	CEF (ST2)	(1)(3)	(Mo)(O)
MoSi2	CEF (SLN)	(1)(2)	(Mo,Nb,W)(Si)

Name	Model	Lattice Size	Constituent
MoSi6Ti2	CEF (SLN)	(1)(2)	(Mo,Ti)(Si)
Mu_Phase	CEF (SLN)	(1)(2)(4)(6)	(Fe,Mo,Nb,Ta,W)(Fe,Mo,Nb,Ta,W) (Fe,Mo,Nb,Ta,Ti,W)(Fe,Mo,Ta,W)
Nb2O5	CEF (ST2)	(2)(5)	(Nb)(O)
Nb3Si	CEF (SLN)	(0.75)(0.25)	(Hf,Nb,Ti,Zr)(Al,Si)
Nb5Si3	CEF (SLN)	(0.625) (0.375)	(Cr,Hf,Nb,Ti,V,Zr)(Al,Si)
Nb9Si2Cr3	CEF (SLN)	(0.643) (0.143) (0.214)	(Nb)(Si)(Cr,Si)
NbO	CEF (ST2)	(1)(1)	(Nb)(O)
NbO2	CEF (ST2)	(1)(2)	(Nb)(O)
Phi	CEF (SLN)	(0.8837) (1.1163)	(Al,Ta)(Al,Ta)
Quartz	CEF (ST2)	(1)(2)	(Si)(O)
R_Phase	CEF (SLN)	(27)(14)(12)	(Fe)(Mo)(Fe,Mo)
Re2O7	CEF (ST2)	(2)(7)	(Re)(O)
Re2Si	CEF (ST2)	(2)(1)	(Re)(Si)
ReO2	CEF (ST2)	(1)(2)	(Re)(O)
ReO3	CEF (ST2)	(1)(3)	(Re)(O)
ReSi	CEF (ST2)	(0.5)(0.5)	(Re)(Si)
ReSi2	CEF (SLN)	(1)(2)	(Re)(Si,Va)
Rutile	CEF (SLN)	(1)(2)	(Ti+3,Ti+4,V+4)(O-2,Va)
Si2Ta	CEF (ST2)	(0.6667) (0.3333)	(Si)(Ta)

Name	Model	Lattice Size	Constituent
Si2Ti	CEF (SLN)	(2)(1)	(Al,Si)(Cr,Mo,Nb,Ti)
Si3Ta5_HT	CEF (ST2)	(0.375) (0.625)	(Si)(Ta)
Si3Ta5_LT	CEF (ST2)	(0.375) (0.625)	(Si)(Ta)
Si3Ti5	CEF (SLN)	(3)(5)	(Si)(Cr,Fe,Hf,Mo,Nb,Ti,V,Zr)
Si5V6	CEF (SLN)	(0.454545) (0.545455)	(Si)(Cr,V)
SiO_AM	CEF (ST2)	(1)(1)	(Si)(O)
SiTa2	CEF (ST2)	(0.3333) (0.6667)	(Si)(Ta)
SiTa3	CEF (ST2)	(0.25)(0.75)	(Si)(Ta)
Sigma	CEF (SLN)	(8)(4)(18)	(Al,Fe,Re,Si,Ta,Ti)(Cr,Fe,Mo,Nb,Ta,V,W) (Al,Cr,Fe,Mo,Nb,Re,Si,Ta,Ti,V,W)
Spinel	CEF (SLN)	(1)(2)(2)(4)	(Al+3,Cr+2,Cr+3,Fe+2,Fe+3) (Al+3,Cr+3,Fe+2,Fe+3,Va)(Fe+2,Va)(O-2)
Ta2O5_S	CEF (SLN)	(1)	(Ta,Ta2O5)
Ta2O5_S2	CEF (SLN)	(1)	(Ta,Ta2O5)
Ti10O19	CEF (ST2)	(10)(19)	(Ti)(O)
Ti20O39	CEF (ST2)	(20)(39)	(Ti)(O)
Ti2Al5	CEF (SLN)	(2)(5)	(Nb,Ti)(Al)
Ti2AlNb	CEF (SLN)	(0.75)(0.25)	(Nb,Ti)(Al)
Ti3Al	CEF (SLN)	(0.75)(0.25)	(Al,Nb,Ti)(Al,Nb,Ti)
Ti3Al2Si5	CEF (ST3)	(1)(0.6)(1.4)	(Ti)(Al)(Si)
Ti3O2	CEF (ST2)	(3)(2)	(Ti)(O)

Name	Model	Lattice Size	Constituent
Ti3O5	CEF (ST2)	(3)(5)	(Ti)(O)
Ti4Al3Nb	CEF (ST3)	(0.5)(0.375) (0.125)	(Ti)(Al)(Nb)
Ti4O7	CEF (ST2)	(4)(7)	(Ti)(O)
Ti5O9	CEF (ST2)	(5)(9)	(Ti)(O)
Ti6O11	CEF (ST2)	(6)(11)	(Ti)(O)
Ti7Al5Si14	CEF (ST3)	(7)(5)(14)	(Ti)(Al)(Si)
Ti7O13	CEF (ST2)	(7)(13)	(Ti)(O)
Ti8O15	CEF (ST2)	(8)(15)	(Ti)(O)
Ti9O17	CEF (ST2)	(9)(17)	(Ti)(O)
TiAl	CEF (SLN)	(0.5)(0.5)	(Al,Nb,Ti)(Al,Nb,Ti)
TiAl2	CEF (SLN)	(1)(2)	(Nb,Ti)(Al)
TiOx	CEF (SLN)	(1)(1)(1)	(Ti+2,Ti+3,Va)(Ti,Va)(O-2)
Tridymite	CEF (ST2)	(1)(2)	(Si)(O)
V2O5	CEF (ST2)	(2)(5)	(V)(O)
V2O_SS	CEF (SLN)	(1)(0.5)	(V)(O,Va)
V2Zr	CEF (ST2)	(2)(1)	(V)(Zr)
V3O5_HT	CEF (ST2)	(2)(1)(5)	(V+3)(V+4)(O-2)
V3O5_LT	CEF (ST2)	(2)(1)(5)	(V+3)(V+4)(O-2)
V3O7	CEF (ST2)	(2)(1)(7)	(V+5)(V+4)(O-2)
V4O7	CEF (ST2)	(2)(2)(7)	(V+3)(V+4)(O-2)
V52O64	CEF (ST2)	(52)(64)	(V)(O)
V5O9	CEF (ST2)	(2)(3)(9)	(V+3)(V+4)(O-2)
V6O11	CEF (ST2)	(2)(4)(11)	(V+3)(V+4)(O-2)

Name	Model	Lattice Size	Constituent
V6O13	CEF (ST2)	(2)(4)(13)	(V+5)(V+4)(O-2)
V7O13	CEF (ST2)	(2)(5)(13)	(V+3)(V+4)(O-2)
V8O15	CEF (ST2)	(2)(6)(15)	(V+3)(V+4)(O-2)
VO2	CEF (SLN)	(1)(2)	(Hf,Mo,V,W,Zr)(O)
WO272	CEF (ST2)	(1)(2.72)	(W)(O)
WO290	CEF (ST2)	(1)(2.9)	(W)(O)
WO296	CEF (ST2)	(1)(2.96)	(W)(O)
WO3_A	CEF (ST2)	(1)(3)	(W)(O)
WO3_B	CEF (ST2)	(1)(3)	(W)(O)
Y2O3_hex	CEF (SLN)	(2)(3)(1)	(Zr+4)(O-2)(O-2,Va)
Zr21Re25	CEF (SLN)	(0.5435) (0.4565)	(Re)(Hf,Zr)
Zr2O	CEF (ST2)	(2)(1)	(Zr)(O)
Zr3O	CEF (ST2)	(3)(1)	(Zr)(O)
Zr6O	CEF (ST2)	(6)(1)	(Zr)(O)
ZrO2_Cubic	CEF (SLN)	(1)(2)	(Hf,Zr)(O,Va)
ZrO2_Tetra-gonal	CEF (SLN)	(1)(2)	(Hf,Zr)(O,Va)